NBSIR 75-740

Piezoelectric Polymer Transducer for Impact Pressure Measurement

Aimé S. DeReggi

Electronic Technology Division
Institute for Applied Technology
National Bureau of Standards
Washington, D. C. 20234

July, 1975

Final Report Covering Period
December 15, 1973 to December 31, 1974

NBSIR 75–740

PIEZOELECTRIC POLYMER TRANSDUCER FOR IMPACT PRESSURE MEASUREMENT

Aimé S. DeReggi

Electronic Technology Division
Institute for Applied Technology
National Bureau of Standards
Washington, D. C. 20234

July, 1975

Final Report Covering Period
December 15, 1973 to December 31, 1974

The development and calibration efforts described in this report are
exploratory in nature and are intended to serve as a basis for further
work. The measurement results reported are derived from a statistically
small number of test transducers, and the conclusions that may be drawn
are therefore tentative.

ABSTRACT

Described are development efforts relating to the design, construction,
and calibration of a piezoelectric polymer transducer for the recording
of pressure transients developed over the interface between two bodies
as a result of impact. A bilaminate design was selected which uses
electrically poled sheets of 25-μm poly(vinylidene fluoride) as the
active material. The intended primary response of the transducer is
to compression in the thickness direction, which is produced by either
hydrostatic or normal pressure; the transducer was also found to respond
to extension in the membrane direction. Individual-sheet activity in
the thickness-compression mode is approximately 15 pC/N, resulting in a
bilaminate transducer pressure response of 4.5 μV/Pa (30 mV/psi).
Instructions for poling sheets and for constructing transducers are given
in detail. Static and dynamic methods for characterizing transducer out-
put are described. In particular, in order to simulate field conditions
in which the transducer may bend or stretch, or both, during impacts, a
drop-test procedure with curved impactors has been devised, and a theoret-
ical analysis (simplified to the extent of considering the membrane-stress
contribution negligible) has been developed to yield the interface
pressure.

Piezoelectric Polymer Transducer
for Impact Pressure Measurement

Aimé S. DeReggi

1. INTRODUCTION

This report describes the development of a pressure transducer design utilizing a polymeric piezoelectric element [1]* for sensing impact-interface pressure. The measurement of interface pressure is of current interest in studying injury sustained in vehicular crashes.

The results of recent impact-injury studies conducted elsewhere and also sponsored by NHTSA [2] have demonstrated a correlation between the interface pressure developed in the impact region and the severity of local injury. These results were obtained in controlled tests in which it was possible to instrument the impacting device in order to establish the maximum pressure developed during impact. In less controlled tests, such as crash tests with anthropomorphic dummies or with human cadavers, it has not been feasible to make reliable interface-pressure measurements with commercially available instrumentation.

A technique for measurement of peak pressures by using dye-filled micro-capsules adhered to a flexible substrate which is placed over the impact surface was studied elsewhere [3]. While this method of pressure gaging yields the spatial distribution of the peak pressure and has the advantage of requiring no electrical connections to the gage, it cannot provide the pressure history.

The pressure history is important in establishing the duration of elevated pressure, as well as in ordering the sequence of events which led to the development of the peak pressure. Simultaneity with other impact observables such as the acceleration of the vehicle may readily be ascertained, and effects of secondary impacts distinguished from those of the primary impact. The pressure history also permits more general correlations to be tested as, for example, whether there exists a correlation between the time-rate-of-change of pressure and the extent of injury.

A pressure transducer made with piezoelectric polymer sheet material not only can provide the pressure history, but also may be made sufficiently thin and flexible to be mounted on curved surfaces. When mounted on human skin or implanted in the body, the polymer material should provide a good acoustical impedance match to skin or flesh because the densities of these materials closely match that of the polymer. As results given in this report demonstrate, prototype sensors have sensitivities approaching those of piezoelectric ceramics, i.e., on the order of 1 µV/Pa (10 mV/psi) for

---

*Figures in brackets refer to references, section 6.

25-μm poly(vinylidene fluoride) (PVF$_2$). The dynamic range of pressure based on the limit imposed by the polymer room-temperature yield stress extends to approximately 40 MPa (6000 psi) in the case of PVF$_2$. Moreover, as the polymer material itself should provide low-Q resonance behavior, a polymer sensor can be designed to exhibit a broad, flat frequency response.

2. OBJECTIVES

The central objective of this program (DOT-HS-4-00835) is to develop a polymeric pressure transducer capable of measuring the interface pressure developed when the surfaces of two bodies of different compliance come together under impact. The range of pressure specified is nominally zero to a maximum of 1.4 MPa (200 psi), and the range of frequency a few hertz to 10 kHz.

The detailed work statement originally called for the development, construction, and pressure calibration of at least ten polymer transducers suitable for mounting on the surface of anthropomorphic dummies for impact studies. The statement also specified that the sponsor would be supplied with ten calibrated transducers sufficiently inert chemically to be suitable for implantation into the brains of sub-human primates. The work statement also called for the construction and test of a prototype sensing network for use on the chest and on the head of an anthropomorphic dummy.

As the work progressed to the pressure-calibration stage, it became clear that the sensitivity of the piezoelectrically active elements to bending and stretching was sufficiently large and difficult to predict as to require separate careful investigation before the transducers should be delivered for use in the field. After a series of discussions between the sponsor and project staff, it was deemed advisable to suspend the development of the pressure-calibration methods for the pressure and frequency ranges specified, and to redirect the work toward defining the types and magnitudes of outputs which can be expected when a transducer is subjected to the imposition of curvature during impact. This change of emphasis in the work was authorized by agreement between the sponsor and the performing organization.

3. EXPERIMENTAL DEVELOPMENT

3.1 Principles Governing Transducer Performance and Design

3.1.1 Piezoelectric Properties - The general relation between electric displacement vector $\underline{D}$, electric field vector $\underline{E}$, and stress tensor $\underline{\underline{T}}$ (a tensor of second rank) is expressed [4] by the matrix equation

$$-D_i + \varepsilon_{ij}E_j + d_{im}T_m = 0 \qquad (ij = 1, 2, 3 \text{ and } m = 1, 2...6), \qquad (1)$$

where summation is implied by the repeated index. In (1), six-element column matrix T_m represents the stress tensor. Conventionally, matrix elements $T_1, T_2,...,T_6$ represent tensor components $T_{11}, T_{22}, T_{33}, T_{23}$,

T_{13}, T_{12} in that order [4]. The elements of 3 x 6 matrix d_{im} represent components of a third-rank tensor. These elements are called piezoelectric strain moduli (with units C/N, equivalent to m/V). The matrix ε_{ij} represents the ordinary permittivity tensor $\underline{\varepsilon}$ (a tensor of second rank).

The relation between $\underline{D}$, $\underline{E}$, and stress-induced polarization vector $\underline{P}$ is

$$D_i = \varepsilon_{ij}E_j + P_i. \tag{2}$$

This equation and (1) show that moduli d_{im} relate polarization components P_i to stress components T_m in the following way:

$$P_i = d_{im}T_m. \tag{3}$$

For a flat sheet of PVF_2 which has electrodes on both sides and which has been poled across the sheet (i.e., in a direction defined as the 3-direction), there exists a frozen-in, poling-field-induced polarization P_3 distinct from P in (3). The charge associated with P_3 tends to become neutralized during poling (by injected charge) or during storage (by stray atmospheric charge). In any case, this polarization charge is not observable in dynamic measurements.

Equation (1) with D = 0 shows that an applied stress induces an electric field, given by

$$E_j = -(\varepsilon^{-1})_{ij}d_{im}T_m = -(\varepsilon^{-1})_{ij}P_j. \tag{4}$$

The product $(\varepsilon^{-1})_{ij}d_{im}$ is another matrix g_{jm}, the elements of which are piezoelectric stress moduli. The d_{im} and g_{jm} moduli are related generally as follows:

$$d_{im} = \varepsilon_{ij}g_{jm}. \tag{5}$$

The units of g_{jm} are V · m/N.

For the flat-sheet geometry above, the relation

$$E_j = g_{jm}T_m$$

implies that an open-circuit voltage will appear across the electrode under applied stress.

The d-matrix for a poled PVF_2 sheet, written out explicitly in rectangular Cartesian coordinates, is [5,6]:

$$d = \begin{bmatrix} 0 & 0 & 0 & 0 & d_{15} & 0 \\ 0 & 0 & 0 & d_{24} & 0 & 0 \\ d_{31} & d_{32} & d_{33} & 0 & 0 & 0 \end{bmatrix}. \tag{6}$$

The d_{33} component determines the response to normal force. The d_{31} and d_{32} components determine the response to membrane forces, i.e., forces acting in the plane of the sheet. In general, d_{31} and d_{32} are not equal, especially if the polymer material was stretched and rolled during the manufacturing process or during the poling process. If stretching has occurred in the 1-direction, $d_{31} > d_{32}$. Recently, PVF_2 sheet material which has been biaxially stretched during manufacture has become available. For this material, and no further stretching during poling, it is expected that $d_{31} \approx d_{32}$. The d_{15} and d_{24} components determine the response to shear stresses. As a rule $d_{33} > d_{31} > d_{32} > d_{15}, d_{24}$ [5,6].

For a given polymer-sheet material, the values of the components of d depend on the poling procedures, that is, on the polarizing field, on the polarizing temperature, and possibly also on the temperature and field histories. Routinely achievable values of d_{33} in this laboratory for 25-μm (0.001 in) sheets of PVF_2 are between 10 and 15 pC/N for the following poling conditions: 800 kV/cm polarizing field, 120°C polarizing temperature, temperature history consisting of first heating to 120°C followed by cooling to room temperature, the total cycle being completed within approximately 30 minutes, and applied field at its maximum value throughout the thermal cycle. Corresponding values of d_{31} are between 5 and 8 pC/N. Precise values for the shear components are not available.

The piezoelectric moduli are not expected to have a significant intrinsic frequency dependence in the frequency range of interest.

The piezoelectric moduli are somewhat temperature-dependent. According to data supplied by the manufacturer, the temperature coefficient of d_{31} for PVF_2 near room temperature is positive and increases in an approximately logarithmic fashion with temperature such that a d_{31} value of 10 pC/N at 20°C becomes 14 pC/N at 50°C. The transducer calibration should therefore include a correction factor for the effect of ambient temperature.

In the foregoing discussion, it has been assumed that the strains imposed upon the piezoelectric element of the transducer are homogeneous. Additional effects associated with real charge (i.e., charge injected during the poling process that becomes trapped in the polymer and is therefore present after poling) are possible if the strains are inhomogeneous [7,8]. Such effects are not considered explicitly in this report.

3.1.2 Electrical Response - The piezoelectric response of a polymer sheet with electrodes on opposite surfaces can be measured with a charge amplifier or a voltage amplifier. A charge amplifier measures the charge which flows in an external circuit to neutralize the stress-induced charge Q appearing on the electrodes. In effect, measurements made with a charge amplifier measure the short-circuit charge in that the electrodes are maintained at the same potential. A voltage amplifier with sufficiently high input resistance measures the open-circuit voltage V appearing across the electrodes.

From Gauss's law and the definition of the piezoelectric modulus g, it follows that

$$Q = \int \varepsilon E \cdot dA = -\int \varepsilon gT \cdot dA, \tag{7}$$

where T is a general component of the stress tensor, E and g are components of the dielectric and piezoelectric tensors appropriate to the stress component T, and where the integration is to be carried out over the surface A of the piezoelectric sheet. In the general case, all components of the T-tensor contribute to Q.

For interface pressure measurements, the primary stress component is T_{33}, the normal stress in the 3-direction. The response associated with T_{33} is a scalar quantity represented by Q_{33}, which is proportional to $\int T_{33} \cdot dA$, which is the total normal force, F_3, applied to the sensitive area. Thus, we have $Q_{33} = -\varepsilon_{33}g_{33}F_3$, and corresponding voltage (a scalar quantity) represented by $V_{33} = -\varepsilon_{33}g_{33}F_3/C$.

The capacitance (C) in the above expression includes the capacitance of the piezoelectric sheet and other capacitances, such as cable capacitances, present in the measuring circuit. If the stray capacitances are neglected, and the sheet capacitance is approximated by the parallel-plate formula, $C = \varepsilon A/t$, where A is the area and t the thickness of the active part, the voltage V_{33} becomes

$$V_{33} = -g_{33}tF_3/A = -g_{33}tP_{av}, \tag{8}$$

where $P_{av} = F_3A$ is the average pressure over the sensitive area of the sheet. Thus given arbitrary distribution of normal pressure acting on the piezoelectric area A, Q_{33} is proportional to the force, and V_{33} to the average pressure.

For a bilaminate transducer with two sheets connected electrically in parallel and mechanically in series, the charge responses of the two component sheets add. The voltage response of the transducer is that of each sheet, assuming that the sheet responses are the same. If they are not, the transducer voltage response is equivalent to the average of the sheet responses.

As the resistivity of PVF_2 before and after poling is of the order of $10^{14}\Omega \cdot cm$, the leakage resistance of a polymer sheet will be very high. In the case of a 1-cm-diameter disk, the resistance is of order $10^{11}\Omega$. With a dielectric constant K of approximately 10, the capacitance will be approximately 1 nF. Hence the source time constant will be of order 100 s. With suitable amplifiers, quasi-static pressure measurements are thus possible. With ordinary a-c charge or voltage amplifiers, the measured response will have a low-frequency roll-off set by the instrumentation rather than by the polymer transducer.

The frequency response in the audio range and beyond will depend on the nature of mechanical resonances. The thickness-compression resonance is in the 1 MHz range, but other modes such as membrane-extension modes may have constraint-dependent resonances at much lower frequencies.

3.1.3 Effects of Membrane Stresses - In those applications in which a transducer is mounted on the surface of a compliant body and adheres to the surface during impact with another body, the transducer active element may be subjected to stretching and bending, in which cases membrane stresses will be generated. Membrane stresses can result in significant contributions to transducer response because relatively small membrane forces produce large membrane stresses in thin transducer elements. For example, in the case of 1-cm-diameter element 25-μm (0.001-in) thick, the area resisting membrane forces is 300 times smaller than the area resisting compressive forces across the sheet due to the external pressure. Thus, the charge outputs resulting respectively from pressure-related compressive forces and from stretching forces will be comparable if the stretching force is 150 times smaller than the compressive force, assuming $d_{33} = 2d_{31}$.

3.1.3.1 Consider first the case of flat impacting surfaces. The impact-induced strains occurring within the impacting bodies along the impact interface where a pressure transducer is located will tend to have components parallel to the interface, with magnitudes in roughly the same proportion to the magnitude of the component normal to the interface, as Poisson's ratio. It follows that if the impacting bodies do not have compliances and values of Poisson's ratio identical to those of the transducer material, additional voltage contributions $V_{31} = Q_{31}/C$ and V_{32}/C will be present in the transducer output and will be respectively proportional to $d_{31}T_{22}$ and $d_{32}T_{22}$, where T_{11} and T_{22} represent mutually perpendicular membrane stresses. If the impacting bodies have a common compliance which is much greater than that of the transducer, then there will be a tendency for the deforming bodies to impart tensile membrane forces to the transducer through frictional forces, or through the bonding material if one is used. The signs of V_{31} and V_{32} will be the same as that of V_{33} since these voltages arise from stresses tending to reduce the thickness of the transducer. As frictional forces on the surfaces of the transducer are difficult to avoid, it may be worthwhile to use lubrication as a means of reducing the coefficient of friction to the lowest possible value and of ensuring that $V_{33} \gg V_{31}, V_{32}$.

3.1.3.2 Case of imparted single curvature. Single curvature is imparted to a transducer mounted on a compliant body when a relatively hard cylindrical object impacts the body (the direction of motion is understood to be normal to the surface of the body before impact, with elements of the impactor cylindrical surface normal to the direction of motion). Membrane forces again will be generated. If bending occurred with negligible frictional forces present over opposite surfaces of the transducer, the neutral surface would remain midway across the thickness of the transducer. The membrane-stress distribution would be antisymmetric with respect to

the neutral surface. Assuming the same d_{31} (and d_{32}) for the transducer material on both sides of the neutral surface, the piezoelectric responses from regions on opposite sides of the neutral surface should cancel to a first approximation. In the presence of frictional forces which are different on opposite surfaces of the transducer, bending would result in a displacement of the neutral surface, a net membrane stress, and a net response to bending. The extent to which lubrication can reduce neutral surface displacement during bending is best determined by experiment. A transducer made with two piezoelectric elements, back-to-back, might have an unbalance related to differences in the d_{31} and d_{32} values of the component elements, and hence could exhibit a response to bending, even if the neutral surface coincided with the contacting surfaces of the component elements. In this case lubrication would not eliminate the net bending response even though it would tend to eliminate the net membrane stresses.

3.1.3.3 Case of imparted double curvature. Double curvature is imparted to a transducer mounted on a compliant body when a relatively hard spherical object impacts the body (the direction of motion is understood to be normal to the undisturbed surface of the body before impact). Membrane stresses are unavoidable, whether or not lubrication is used. To reduce the bending response in such cases, it may be advantageous to reduce the area of the transducer element. As the voltage output in response to pressure of a transducer element does not depend on sensing area, a negligible reduction in voltage output will result, provided the stray capacitance is small compared to the capacitance of the transducer element. The effects of double curvature with and without lubrication are probably best determined by experiment. A similar comment applies even more strongly for more general compound curvature.

3.2 Transducer Construction

The following step-by-step procedure details the construction of a typical polymeric pressure transducer. This procedure produces bilaminate transducers in lots of nine.

(1) Two rectangular sheets, 13 cm x 16 cm, are cut from a roll of capacitor-grade PVF_2 sheet 25-μm thick.

(2) Each sheet of PVF_2 is sandwiched between two sheets of glass. This assembly is placed in an oven and is heat-treated at 130 ±10°C for approximately two hours. This annealing treatment serves to reduce permanent and severe dimensional changes during subsequent steps.

(3) On one side of each sheet (referred to as the electrical high side) a mask-defined pattern of nine identical aluminum electrodes, as shown in figure 1, is deposited by evaporation in a vacuum chamber. The pattern is defined by an evaporation mask which is also shown in figure 1. Aluminum was selected as the electrode material because it is easy to evaporate, adheres well to the polymer substrate, and has good electrical

conductivity in thin-film form. Each electrode consists of a 1-cm-diameter circular area connected to a 0.2-cm-diameter circular dot by a strip 10.1-cm long and 0.04-cm wide. The 1-cm-diameter spot defines the area which ulti- mately becomes active; the strip serves as an electrical lead, and the small dot as a pad for later electrical connection to the center conductor of a low-noise cable. The nine electrodes are deposited side-by-side, so that the nine strip leads are parallel and 1.6-cm apart, while the 1-cm-diameter spots and the 0.2-cm-diameter pads form respective parallel linear arrays, nominally 10 cm from each other. Approximately 0.2 μm of aluminum is deposited, which results in a strip lead resistance of less than 100 Ω.

(4) On the opposite side of each sheet a strip electrode, 3-cm wide and approximately 0.1-μm thick, is deposited in line with the array of 1-cm- diameter dots. During poling, this strip serves as a common electrical ground electrode. Figure 1 shows how this strip is oriented.

(5) Each sheet, together with two strips of tin foil for electrical con- tact to the exterior, is then sandwiched between two insulating sheets of 250-μm-thick polyethylene terephthalate. One tin-foil strip contacts the common ground electrode, and the other contacts all nine high-side leads. This assembly is mounted between the 23 x 23-cm platens of an hydraulic hot press, and a load of approximately 40 kN (four-tonf gage reading) is applied. The positive output terminal of a high-voltage d-c power supply is connected to the high electrode, and the negative terminal is connected to the ground electrode. The steel frame of the press and the negative terminal of the power supply are connected to laboratory ground. A poling voltage of 2000 ±50 V is applied, corresponding to a field of about 8 x 10^5 V/cm across the polymer in the region defined by the 1-cm-diameter areas. The PVF$_2$ is heated to a temperature of 120°C, as measured by a thermocouple inserted between the insulating sheets, and cooled immediately thereafter to room temperature. The heating part of the cycle takes approximately 20 min and the cooling part approximately 15 min. This procedure poles the PVF$_2$ selectively in the regions of the 1-cm areas, and leaves the nine strip- leads effectively inactive. Pressure is applied during poling to prevent wrinkling of the polymer sheets under the combined effects of field and temperature.

(6) After removal from the press, an aluminum shield electrode, 0.1-nm thick, is deposited on the ground side of each sheet, extending the ground electrode to cover nominally the entire surface of that side of the sheet. To avoid depoling the nine activated areas during this evaporation, which heats the polymer substrate, the part of the ground electrode used during poling consisting of a 1.5-cm-wide strip opposite the set of 1-cm-diameter dots, and aligned with them, is masked off by a metal strip. Another strip, also 1.5-cm wide, masks off another area, opposite the set of 0.2-cm-diameter dots on which it is centered to provide a clear area for visual alignment of one sheet with another in a later step.

(7)   The high side of each sheet is then coated with a thin layer of contact cement* by wiping the surface with a foam-rubber pad saturated with a solution of contact cement diluted 5 to 1 with toluene. The contact cement is allowed to dry at least 15 min to allow the solvent to evaporate.

(8)   Nine pieces of 250-μm-diameter, tinned-copper wire are cut to a length of 5 cm, and one end is flattened over a length of approximately 0.6 cm, by rolling the end in a bench-type rolling mill. The flattened portions of the nine wires are coated with a thin layer of silver-bearing epoxy and are laid on the nine high leads of one of the sheets, in a manner such that the flattened portion contacts the 0.2-cm-diameter dots at the ends of the evaporated leads. A small drop of contact cement is then applied to each wire immediately behind the flattened portion to form a fillet for the round wire and to hold the wire in place on the sheet.

(9)   The two sheets are precisely positioned on separate, mating, vacuum-hold-down plates with the high, cement-coated, sides facing out. At the same time, they are stretched lightly to make them lie as flat as possible. The plates are then mated so that the cement-coated sides are pressed together to form a bilaminate assembly. Care must be exercised prior to and during this step to insure that when the sheets are bonded, the pattern of dots and leads on one sheet is in satisfactory alignment with the corresponding pattern on the other sheet, and that trapping of air bubbles is minimized. The assembly is then placed in the hydraulic press and further pressed under a load of approximately 250 kN (25-tonf gage reading).

(10)   The bonded sheets are then cut to yield nine separate bilaminate transducer elements. A 12-μm layer of unpoled PVF_2 is then cemented on each side of the elements, covering all but the small portion of the shield electrode at the end where electrical contact is to be made. These layers act as a protective coating to prevent damage to the shield electrode.

(11)   The wire lead of each element is trimmed to leave approximately 0.3 cm protruding outside the polymer sheets. This lead is then soldered to the center conductor of a female miniature bulkhead coaxial connector. Care is taken not to damage the connection to the evaporated lead by excessive soldering heat conducted by the wire.

(12)   The exposed parts of the high lead between the connector and the end of the transducer not covered by the shield electrode are potted in epoxy. After the epoxy has hardened, electrical contact between the shield side of the connector and the shield side of the transducer is made by applying a thick coat of liquid, silver-bearing rubber, over the insulating epoxy and the area surrounding it.

---

*Considerable experimentation was conducted with various bonding agents. Contact cement meeting Federal Specification MMM-A-130a has been satisfactory.

A well-made transducer has a high leakage resistance (usually greater than 10^{11} Ω) and a capacitance of roughly 1 nF. The capacitance of the lead between the active area of the transducer and the coaxial connector contributes only about 10% of this capacitance.

3.3 Transducer Testing and Calibration

3.3.1 Guiding Principles - The preliminary transducer parameter used to characterize performance is pressure sensitivity. The pressure range of interest is from nominally zero (or preferably slightly negative pressure) to 1.4 MPa (200 psi), and the frequency range of interest from approximately 5 Hz to 10 kHz. However, in view of the transducer sensitivity to membrane stresses as well as to pressure, it was felt that a pure-pressure calibration would be of limited value unless an evaluation of all the important contributions to transducer response was made. Further, the evaluation should take account of conditions anticipated in crash studies, in which bending of the transducer may occur in combination with compression. Another guideline was that a transducer intended for use under impact conditions should be tested under impact conditions.

3.3.2 Test and Calibration Methods Considered - The following quasi-static and dynamic methods were evaluated in the process of selecting calibration and test procedures:

(1) Static uniaxial compression produced by means of a small mechanical press,
(2) Sinusoidal compression produced by means of a vibration exciter with a rigid inertial loading mass (to generate periodic variations in pressure),
(3) Sinusoidal hydrostatic pressure generated by a vibration exciter and a liquid column,
(4) Shock tests using a drop-testing machine, and
(5) Shock tests using a miniature shock tube.

Methods (1) and (4) were selected because they have the advantage over other methods that they can produce pressures over the entire range of interest (except for slightly negative pressures). In addition, measurements made on the press and the drop-testing machine were not significantly affected by electrical noise or by 60-Hz pick-up. Methods using vibration exciters available to the project could have achieved pressures only a small fraction of the specified maximum and been useful over only the lower half of the specified frequency range. [Exploratory measurements were made of the frequency response using method (2). The absolute response at any given frequency depended on the bonding agent used to hold the transducer to the vibration-exciter table and the inertial mass to the transducer. The regular use of a rigid bonding agent was precluded by the desirability of recovering the transducer without damage.]

The shock-tube methods were not considered after preliminary tests resulted in anomalously high transducer outputs attributed provisionally to pyro-electric response and surface charging by ions carried in the compressed gas.

3.3.3 *Mechanical Press* - Figure 2 shows the experimental arrangement of the mechanical press. The transducer under test rests on the upper surface of a cylindrical block with plane, parallel upper and lower surfaces. This block is rigidly fastened to a commercial force transducer, which has a measuring range of -440 to +440 N (-100 to +100 lbf). A flat-faced, cylin-drical nylon rod 1.2 cm in diameter is placed over the transducer to cover the entire 1-cm-diameter sensitive area. This rod serves as a mechanical coupler between the polymer transducer and the ball-tipped drive screw.

In operation, the drive screw is manually advanced and withdrawn, varying the uniaxial compression of the polymer transducer along its thickness (i.e., along the 3-direction). An x-y recorder plots the output of the force transducer on the x-axis and the amplified output of the polymer transducer on the y-axis. The amplifier used for most tests is an elec-trometer, and thus transducer charge output is the quantity normally measured.

Figure 3 shows plots for two transducers. The pressure offset is due to a preload applied to smooth out wrinkles in the transducer before the short-ing switch of the charge amplifier is released. The slope of the curves, which is not sensitive to initial charge or to initial pressure, is used to obtain the pressure sensitivity of the transducer. This sensitivity is reproducible from day to day to within a few percent. The range of sensi-tivity among a large number of transducers, however, was found to be unexpectedly broad, as discussed in 4.1.

3.3.4 *Drop Test*

3.3.4.1 Figure 4 shows the overall experimental arrangement for the drop tests. (The drop-testing machine shown in the photograph is a modifica-tion of the commercially available instrument used in this work. Modifi-cations were carried out after the work described here was completed and are therefore not described.) A commercial accelerometer, screwed to the upper face of the dropping carriage, records acceleration as a function of time for each drop. The accelerometer response is specified by the manufacturer as 7.9 mV/g_n over a frequency range of 5 Hz to 15 kHz. Figure 5 shows the selection of interchangeable rigid impactors which are fastened, by means of bolts, to the lower face of the carriage. Each impactor is designed to impart a given shape to the transducer under test during the time at impact that interface pressure is generated between impactor and the compliant pad fastened to the base of the drop tester. As the various impactors have different masses, the total dropped mass depends on the impactor used. Precise values for these masses are given in table 1.

The recording electronics consists of a two-channel transient recorder, a monitor oscilloscope, and an X-Y_1-Y_2 plotter. A charge-sensitive amplifier was sometimes used between the transducer under test and the transient

recorder. These instruments are shown in figure 4. In normal operation, the polymer output and the carriage accelerometer output are recorded simultaneously. However, in order to relate the accelerometer signal to the interface pressure for the various impactors, the penetration depth of the impactor into the pad must also be recorded. This measurement is performed separately with an eddy-current proximity sensor, which can be positioned vertically and horizontally by means of a micrometer-driven stage. In use, the sensor is positioned low enough so that the bottom of the carriage cannot hit it at the lowest point of carriage travel.

Simultaneous records are made (using the transient recorder) of the outputs of the proximity sensor and of the accelerometer in a series of drops in which the proximity sensor is raised in small increments until the recorded signal indicates incipient contact. As figure 6 illustrates, the slightest contact produces an easily resolved flat spot on the proximity-sensor record, when the rms voltage becomes zero. The micrometer reading is recorded at this point and also at the point when the impactor just comes into contact with the pad as the carriage is slowly lowered by hand. The difference between the two readings provides the peak penetration depth with a resolution of ± 25 μm (± 0.001 in). The absolute error is estimated to be no more than ± 130 μm (± 0.005 in). This error is principally due to the inherent limited accuracy with which it is possible to define initial contact between impactor and pad and the mechanical relaxation time of the pad after impact. The full recorded trace represents carriage displacement as a function of time. Because the penetration depths chosen for tests (on the order of 1 cm) far exceed the linear range of the proximity sensor (2 mm), the recorded trace is highly non-linear at separations between carriage and proximity sensor exceeding a few millimeters.

To date, the main use which has been made of the simultaneous records as a function of time of the outputs of the proximity sensor and the accelerometer has been to ensure that peak acceleration occurred at peak penetration. A similar comment applies to the simultaneous records of the outputs of the polymer transducer and the accelerometer. Once it was determined that peak transducer output occurred at peak acceleration, only peak values were analyzed in detail. The general features of the acceleration levels and penetration depths for various impactors as a function of drop height are shown in figures 7 and 8 for a 2.5-kg (5.5-lb mass) carriage and for the flat-surfaced half-sine pad supplied by the manufacturer. This pad was used only in the earlier work, because its construction (three layers of different thicknesses with two different compliances) unnecessarily complicated the theoretical analysis used to relate the dynamic quantities measured to the interface pressure developed. This pad was subsequently replaced by a homogeneous, small-pore, foam-rubber pad, which also had a flat surface. Time limitations did not permit a complete set of measurements to be taken for this pad. The method of mounting the polymer transducer to the pad, which normally involves a few layers of double-sided adhesive tape, affects the detailed mechanical response of the pad (as manifested in the measured penetration depth) for small drop heights which proved useful. Because of the presence of factors affecting the measurement, such as those introduced by the transducer

mounting, measurements for a given transducer normally all were made under the same conditions and during the same period. Drop height could not be varied arbitrarily because, for a given pad and impactor, the drop height had to be adjusted so that the penetration depth was smaller than the impactor radius of curvature but deep enough (1) to impart the curvature of the impactor to the entire sensitive area of the transducer under test and (2) to develop interface pressures in a realistic range.

3.3.4.2 Drop-Test and Calibration Procedure - The following test and calibration procedure was devised to characterize the dynamic response of the polymer transducer when bending with <u>single curvature</u> occurs in combination with compression. The procedure involves two series of tests, normally carried out at constant drop height.

For each series, the imparted radius of curvature is varied systematically, through the use of one flat impactor and either two or three cylindrical impactors. The first series is run with the transducer mounted flat on the pad between two sheets of polytetrafluoroethylene, with ethylene glycol used as lubricant. The second series is run identically, except that the transducer is turned over.

The difference between the outputs of the transducer in the face-up and face-down tests, which was found to vary greatly among transducers, is interpreted as the bending-induced response of the transducer related to unbalance in the piezoelectric properties of the two component sections of the piezoelectric element. This difference in outputs was found to decrease with increasing radius of curvature at constant drop height.

The average of the face-up and face-down outputs is interpreted as the transducer pressure response with an additive term resulting from tension (which causes the polymer to stretch in the direction normal to the axis of the cylindrical impactor). This average value also decreases with increasing radius of curvature at constant drop height. The observed decrease results from both a decrease in interface pressure, as the theoretical analysis of 3.3.5 shows, and a decrease in the magnitude of the tension term. Figure 9 shows illustrative plots of peak output signals of both transducer and accelerometer as a function of inverse imparted radius of curvature.

In principle, a similar test and calibration procedure could be performed to characterize the dynamic response of the transducer when bending with double curvature occurs in combination with compression. Such tests would require spherical, rather than cylindrical, impactors with different radii of curvature. These impactors are available, as well as the theoretical analysis required to determine the interface pressure. However, time did not permit extensive tests to be carried out. One test was conducted to compare the results for a spherical impactor with a large radius to the results for a flat impactor.

3.3.5 Theoretical Analysis for Interface Pressure in Drop Tests - The
theoretical analysis given below develops relationships between interface
pressure and the two measured dynamic variables (the acceleration and maxi-
mum penetration depth) for three impactor-face geometries: flat, spherical,
and cylindrical, as shown in figure 10.

For the analysis, the impactors in figure 10 are assumed to have penetrated
to maximum depth. The penetration depth d refers to the penetration depth
at the center of impact. The interface boundary is assumed to be a circle
of radius a for the flat impactor, a circle of radius r_{max} for the spherical
impactor, and a rectangle of dimensions x_{max} by ℓ_1 for the cylindrical
impactor. In the case of flat and spherical impactors, the interface pres-
sure is P(r), a function of position coordinate r of the set of cylindrical
coordinates { y, r, ϕ } with the y-axis pointing in the vertical direction.
In the case of cylindrical impactors, the interface pressure is P(x), a
function of position coordinate x of the set of rectangular Cartesian
coordinates { x, y, z } with the y-axis again pointing in the vertical
direction, which is perpendicular to the generator of the cylindrical sur-
face of the impactor. The above coordinates are spatial coordinates as
opposed to the coordinates { 1, 2, 3 } used in the discussion of piezo-
electric properties, which are material coordinates.

The theory is based on the underlying assumption that the interface pressure
P(r) or P(x) at any point on the interface is proportional to the impactor
penetration depth $\delta(r)$ or $\delta(x)$ at the same point measured vertically from a
reference plane formed by the upper surface of the pad before impact. The
assumption represents an approximation which reduces the otherwise difficult
actual wave-mechanical problem to a problem which is solvable in closed form.
The actual pad-stress-distribution problem is difficult even if wave effects
are neglected. In that case, the problem reduces to a three-dimensional
elasticity problem, the solution of which requires specification of boundary
conditions over the entire surface of the pad, including the interface. The
specification of realistic strain boundary conditions over the interface is
greatly complicated by poor knowledge of the degree of involvement of static
and sliding frictional forces. Hence the boundary conditions are most poorly
known in the region where the stress distribution is sought.

From the starting assumption, it follows that

$$P(r) = K\ \delta(r) \quad \text{for flat or spherical impactor, or} \qquad (9)$$

$$P(x) = K\ \delta(x) \quad \text{for cylindrical impactor,} \qquad (10)$$

where the proportionality factor K (different for each impactor) is indepen-
dent of δ for a particular d. An explicit dependence of K on d is not
excluded. The numerical value of K is expected to depend not only on
properties and dimensions of the pad material, such as E/ℓ_0 where E is an
elastic modulus and ℓ_0 the thickness of the pad, but also on the impactor
geometry, which determines the strain distribution within the pad and
hence the degree of material containment against flow in the horizontal

plane. For example, the pad is expected to appear softer to a curved impactor than to a flat impactor because the pad material near the center of impact has more freedom to flow radially outward in the former case than in the latter case. In this theory, it is not necessary to know the detailed relationship of K to pad properties and impactor geometry because K can be expressed in terms of experimentally measured quantities as discussed below.

The penetration function $\delta(r)$ or $\delta(x)$ depends on the maximum penetration depth d, but otherwise is a purely geometric function determined by the impactor geometry. Referring to the three cases in figure 10, the penetration function is

$$\delta(r) = d \qquad\qquad \text{for the flat impactor,} \qquad (11)$$
$$\delta(r) = d - R + \sqrt{R^2 - r^2} \qquad \text{for the spherical impactor, and} \quad (12)$$
$$\delta(x) = d - R + \sqrt{R^2 - x^2} \qquad \text{for the cylindrical impactor,} \quad (13)$$

where d is the maximum penetration depth and R the radius of curvature of the impactor and deformed pad. The interface pressure or pad-reaction pressure is then

$$P(r) = Kd \qquad\qquad \text{flat,} \qquad (14)$$
$$P(r) = K (d - r + \sqrt{R^2 - r^2}) \qquad \text{spherical, and} \qquad (15)$$
$$P(x) = K (d - r + \sqrt{R^2 - x^2} \qquad \text{cylindrical.} \qquad (16)$$

The integral over the interface area of the vertical component of the differential contribution to the pad reaction force $dF_{-y} = (\underline{P} \cdot d\underline{S})_{-y}$ gives the total pad reaction force F_{-y}, which, by Newton's law of inertia, is the product of the dropping mass m and the acceleration $\ddot{y}$. This integral is equivalent to the integral $\int P \, dS_h$, the horizontal projection of the differential element of area dS. Hence,

$$F_{-y} = 2\pi \int_0^a P(r) \, r \, dr = m\ddot{y} \qquad \text{flat,} \qquad (17)$$
$$F_{-y} = 2\pi \int_0^{r_{max}} P(r) \, r \, dr = m\ddot{y} \qquad \text{spherical, and} \qquad (18)$$
$$F_{-y} = 2\ell_1 \int_0^{x_{max}} P(x) \, dx = m\ddot{y} \qquad \text{cylindrical,} \qquad (19)$$

where a and r_{max} are the radii of the impact circles for the flat case and for the spherical case, respectively, and where x_{max} is half the maximum value of the x-dimension of the impact rectangle and ℓ_1 its other dimension for the cylindrical case. By geometry, $r_{max} = x_{max} = \sqrt{2Rd - d^2}$.

The quantities d and $\ddot{y}$ are measured dynamic variables. Substituting for P(r) and P(x), performing the integration, and solving for K, it follows that

$$K = \frac{m\ddot{y}}{\pi a^2 d} \qquad\qquad \text{flat,} \qquad (20)$$

$$K = \frac{m\ddot{y}}{2\pi \left\{ (d - R) \dfrac{r_{max}^2}{2} + \dfrac{1}{3} \left[R^3 - (R^2 - r_{max}^2)^{3/2} \right] \right\}} \qquad \text{spherical, and} \quad (21)$$

$$K = \frac{m\ddot{y}}{\ell_1 \left[R^2 \sin^{-1} \dfrac{x_{max}}{R} - (R - d) x_{max} \right]} \qquad \text{cylindrical.} \quad (22)$$

The maximum pressure sampled by a transducer with dimensions small compared to the imparted radius of curvature is approximately P(0), the pressure at the center of the impact surface (i.e., at r = 0 or x = 0). Combining the results of (14), (15), and (16) and (20), (21), and (22) evaluated at r = 0 or x = 0, yields:

$$P(0) = \frac{m\ddot{y}}{\pi a^2} \qquad\qquad\qquad \text{flat,} \qquad (23)$$

$$P(0) = \frac{m\ddot{y}d}{2\pi \left\{ (d - R) \dfrac{r_{max}^2}{2} + \dfrac{1}{3} \left[R^3 - (R^2 - r_{max}^2)^{3/2} \right] \right\}} \qquad \text{spherical, and} \quad (24)$$

$$P(0) = \frac{m\ddot{y}d}{\ell_1 \left[R^2 \sin^{-1} \dfrac{x_{max}}{R} - (R - d) x_{max} \right]} \qquad \text{cylindrical.} \quad (25)$$

The formal range of validity of the last two formulas is that for which d/R ≤ 1. However, in practice, the formulas are expected progressively to lose accuracy as d/R approaches 1, because the membrane forces which have been neglected have negligible vertical components only when d/R << 1.

Figure 11 shows the interface pressure at the center of the impact surface as a function of the imparted radius of curvature for the case of cylindrical impactors. These curves were obtained using (25) with the acceleration and penetration-depth data of figures 7 and 8 and with the masses given in table 1. The curves are shown in the range d/R ≤ 1 but, as indicated above, they are expected to be most realistic physically in the range d/R << 1. A few constant-d/R contours are also included in the figure.

A comparison of figure 9 with figure 11 suggests that a large part of the dependence on radius of curvature observed experimentally for the output of the polymer pressure transducer may be attributed to a systematic variation of the interface pressure. The dependence of the pressure on the impactor curvature comes partly from variation of the interface contact area, and partly from variation of the pressure distribution.

4. RESULTS AND DISCUSSION

4.1 Mechanical Press Test Method

Table 2 shows the d-c pressure sensitivity obtained in the mechanical press for 20 polymer pressure transducers in order of increasing sensitivity. (The

first four entries in table 2 are representative of the sensitivity levels obtained early in the program, while the last ten entries represent sensitivity levels achieved toward the end of the program.) The d-c sensitivity is expressed by the modulus d_{33}^*, which is defined as the induced charge per unit normal force applied to the sensitive area of the transducer, with the top and bottom surfaces of the transducer constrained in a manner specific to the apparatus and to the transducer-mounting method. Apparatus details are specified in 3.3.3. The mounting method consisted of placing each transducer between and in direct contact with the nylon coupler on one side and the aluminum flat on the other, taking care that the coupler face contacted the entire sensitive area of the transducer. No lubrication or bonding agent was used. In obtaining d_{33}^*, it was assumed that the piezoelectric region is confined to a circle of 1-cm diameter. In fact, fringe effects may cause the effective electrode to extend 1 or 2 mm beyond the 1-cm-diameter circle. No correction was made for fringe effects. The highest d_{33}^* listed in table 2 is approximately twice as great as the maximum d_{33} values quoted elsewhere in this report. This is expected because the two sections of a given bilaminate transducer are mechanically in series and electrically in parallel, and hence their charge outputs add. More quantitative comparisons between d_{33}^* and $2d_{33}$ are not appropriate since the relationship between the two quantities, which is not general, was not worked out for the specific conditions of the press-test. Significant differences can be expected between $d_{33}^*/2$ and d_{33}, since $d_{33}^*/2$ is measured on a specimen in the form of a sheet, while the conventional method of measuring d_{33} employs specimens in the form of a needle.

4.2 Drop Tests

4.2.1 Single Curvature Imparted to Transducer - Table 3 summarizes the results of a series of drop tests performed on a polymer transducer with a large sensitivity to bending. The transducer was sandwiched between two thin polytetrafluoroethylene sheets with ethylene glycol as lubricant. The sandwich was mounted flat on a homogeneous foam-rubber pad by means of double-sided adhesive tape. All drops were done at the same nominal drop height of 25 cm (10 in). Three impactors were used, a flat and two cylindrical impactors, giving radii of curvature of ∞, 2.54, and 1.27 cm (∞, 1.00, and 0.50 in), respectively. The impactor with the smallest radius of curvature of 0.63 cm was found to produce a d/R of approximately unity at the drop height of 25 cm (10 in) and hence was not used. The measured quantities, transducer outputs with side 1 facing up and with side 2 facing up, acceleration, and penetration depth, have been plotted as functions of inverse imparted radius of curvature R^{-1} in figure 9.

The "footprint area" shown in the table is the area of the horizontal projection of the interface area obtained by calculation for each impactor using the measured penetration-depth. The "average pressure over footprint area" is obtained by dividing the decelerating force supplied by the pad ($m\ddot{y}$) by the footprint area. The "calculated pressure at center of footprint" is the pressure obtained using (23) and (25). The

"calculated pressure sensitivity" is the sensitivity obtained by dividing the measured charge output by the calculated pressure. A transducer which is highly responsive to normal pressure and weakly responsive to membrane stresses would have a pressure sensitivity which is insensitive to the imparted radius of curvature. A bilaminate transducer with component sections matched elastically and piezoelectrically would have the same response whether side 1 or side 2 is facing up.

The differences in sensitivity between the side 1-up and side 2-up cases reveal the high degree of mismatch in the elastic and piezoelectric properties, or both, of the component sections of the particular transducer tested. This result points up the need for careful matching of component sections as a part of the transducer construction procedure.

The fact that a sensitivity difference is found between the side 1-up and side 2-up cases with the flat impactor is believed to indicate the existence of a residual contribution to the output related to membrane forces. This observation indicates that, even when the flat impactor is used in conjunction with lubrication, the dynamic stress distribution imposed to the transducer is more complicated than purely uniaxial.

The calculated pressure sensitivity as a function of imparted radius of curvature (last row of table 3) remains constant to within approximately 25 percent while the radius is varied as shown. This result is in contrast with the transducer output, which has a much stronger dependence on imparted radius (rows 3 and 4).

With due consideration given to possible inadequacies in the theory used to obtain the interface pressure, it appears that the transducer ouptut for the geometries tested follows rather closely the interface pressure, which is very sensitive to the impactor geometry. Other measurables, such as the impactor/carriage acceleration, are not so closely related to the interface pressure. The remarks above, of course, underscore the need for a pressure transducer at each point of interest in a crash study.

4.2.2 *Spherical Curvature Imparted to Transducer* - Table 4 compares the results of drop-tests performed with a flat and with a spherical impactor on a polymer transducer with negligible mismatch of its component sections. This transducer also had much greater piezoelectric activity than the transducer used in obtaining the data in figure 9 and table 3. The transducer mounting conditions and drop height are the same as those given as part of the preceding discussion of table 3. Because the voltage output rather than the charge output was measured in this case, the outputs in table 4 are expressed in volts.

The last row of table 4 shows calculated sensitivities for the flat and curved impactors to be in agreement within 7 percent. This agreement suggests that the measured significant difference in output between the flat and curved case (row 2) reflects the difference in interface pressure in the two cases and not effects associated with imparting double curvature.

The exploration of a range of imparted spherical curvature was left for future study.

There is a problem in performing tests with much greater spherical curvature, which is that wrinkling of the surface of the transducer occurs, particularly around the edges. Such wrinkling was found to occur with 2.5-cm (1-in) radius ball-impactors. Since the theory developed in this report assumes that the shape imparted to the transducer is the shape of the impactor, the theory is applicable only for moderate imparted spherical curvature.

5. SUMMARY AND RECOMMENDATIONS

A polymer-sheet pressure transducer, operated in the thickness-compression mode, has been developed for impact interface-pressure measurements. The selected design is of bilaminate construction. Two piezoelectric polymer elements are bonded high side to high side in such a manner that the inner faces in mutual contact form a common positive electrode and the outer faces form a negative shield electrode. To make electrical connection to the transducer element, the positive electrode is connected to the center conductor of a coaxial cable and the shield electrode is connected to the cable shield, which is normally grounded. This construction is appropriate for the very high source resistance of the transducer, in that it provides electrical screening of the sensitive part of the source circuit while permitting connection to a single-ended signal line compatible with the input circuitry of commercially available high-input-impedance amplifiers. As the two transducer elements are mechanically in series by virtue of the bilaminate construction, but electrically in parallel, the charge outputs of the component elements add, but the voltage outputs do not.

5.1 Transducer Sensitivity

The sensitivity of the polymer transducer to pressure satisfies the sponsor's requirements.

The piezoelectric constant d_{33} has been increased from about 5 pC/N (22 pC/lbf) to about 15 pC/N (22 pC/lbf) by means of improved poling techniques. This increase, translated into transducer pressure sensitivity, represents an improvement from 1.5 to 4.3 μV/Pa (10 to 30 mV/psi) for 25-μm-thick PVF_2.

5.2 Transducer Frequency Response

The frequency response of the transducer also satisfies the requirements given by the sponsor for the intended interface-pressure measurements. The low-frequency roll-off point is set by the amplifier to be around 1 Hz, while the high-frequency response should be primarily limited only by the thickness-resonance frequency, which is estimated to be a few megahertz. Deviations from a flat response in the range of pressures of interest for crash studies are expected only if imperfections in the transducer piezoelectric material

or transducer construction introduce lower frequency resonances or lower
the thickness-resonance frequency, or if the transducer is tested or used
in a manner which excites modes other than the thickness-compression mode.

5.3 Test Methods for Measuring Transducer Output

Two basic test methods for measuring transducer output have been developed.
The first method uses a mechanical press for static calibration of trans-
ducer output under conditions approximating uniaxial compression. The
second method uses a drop-test machine for measurement of transducer output
under conditions in which pressure and flexure are simultaneously applied.
Because of time limitations, only the effects of imparting single curvature
to the transducer at impact have been studied in detail.

The results of drop-tests with cylindrical impactors of various radii of
curvature indicate that membrane stresses can introduce significant contri-
butions to transducer output mixed with the output resulting from applied
pressure. However, these results also indicate that if lubrication is
used to reduce frictional forces between transducer and the compliant body
to which it is attached, extraneous outputs arising from membrane stresses
may be held to acceptably low levels in all but extreme cases.

5.4 Recommendations for Further Work

The following recommendations are presented for future work:

(1) The effects of spherical curvature imparted to the transducer during
impact should be investigated experimentally and theoretically with and
without lubrication. The imposition of spherical curvature to a nominally
flat transducer results unavoidably in the generation of a membrane stress
distribution, which will be specific to each impact. For this reason, it
should be advisable to explore a range of experimental conditions closely
simulating particular classes of conditions expected during motor-vehicle
crashes.

(2) The effects of transducer size should be investigated. Theoretical
considerations indicate that the effects of bending, both with single and
spherical curvature, will become less important as the size of the transducer
is reduced.

(3) Compound piezoelectric-element designs should be explored such as a
transducer with two separate concentric sensitive areas, in the form of a
central dot and an annulus surrounding the dot. The separate sections of
such transducers would have different sensitivities to bending and should
allow estimates to be made of the accuracy of the pressure measurements
in the presence of bending stresses.

(4) An evaluation of the polymer pressure transducer should be made for
applications involving fluid pressures, to permit measurements such as
intracranial fluid pressure measurements during impact.

6. REFERENCES

[1] Cohen, J., and Edelman, S., Piezoelectric Effect of Oriented Polyvinyl-chloride and Polyvinylfluoride, J. Appl. Phys. 42, 3072-3074 (July 1971).

[2] Contracts FH-11-72888 and DOT-HS-031-2-382.

[3] Contract DOT-HS-024-2-490.

[4] Berlincourt, D.A., Curran, D.R., and Jaffe, H., Piezoelectric and Piezomagnetic Materials and Their Function in Transducers, Book, Physical Acoustics, Vol. 1, Part a., Ed. W.P. Mason, pp. 169-270 (Academic Press, New York, NY, 1964).

[5] Fukada, E., and Takashita, S., Piezoelectric Effect in Polarized Poly(vinylidene Fluoride), Japan, J. Appl. Phys. 8, p. 960 (1969).

[6] Kawai, H., The Piezoelectricity of Poly(vinylidene Fluoride), Japan, J. Appl. Phys. 8, pp. 975-976 (1969).

[7] Hayakawa, R., and Wada, Y., Piezoelectricity and Related Properties of Polymer Films, Book, Advances in Polymer Science, Vol. 11, Ed. H.J. Cantow, *et al*, pp. 1-55 (Springer-Verlag, New York, NY, 1973).

[8] Nakamura, K., and Wada, Y., Piezoelectricity, Pyroelectricity, and the Electrostriction Constant of Poly(vinylidene Fluoride), J. Polymer Sci. A-2, 9, pp. 161-173 (1971).

Table 1

Drop Masses for 2.5-kg Carriage

Impactor Identification	Impactor Geometry	Total Mass Dropped (kg)
A	Flat	2.562
B	Spherical, with radius of curvature of 25 cm. This impactor was furnished with the drop-tester.	2.592
C	Cylindrical, with radius of curvature of 2.5 cm (1.0 in).	2.530
D	Cylindrical, with radius of curvature of 1.25 cm (0.50 in).	2.336
E	Cylindrical, with radius of curvature of 0.62 cm (0.25 in).	2.382

Table 2

Six-Trial Pressure Sensitivity, d_{33}^*, of 20 Transducers
as Measured with the Mechanical Press Apparatus

Mean (pC/N)	Sample Standard Deviation (pC/N)
5.2	0.1
5.3	0.1
5.4	0.1
5.6	0.3
15.1	0.3
20.6	0.5
22.8	0.6
23.5	1.1
24.5	2.1
25.2	0.4
25.3	1.2
26.1	0.4
26.3	0.6
26.5	0.9
26.6	1.1
27.0	0.8
27.2	0.7
27.7	0.6
28.2	0.5
28.9	0.8

Table 3

DROP TEST CONDITIONS AND DATA FOR SINGLE POLYMER PRESSURE TRANSDUCER EVALUATED WITH ONE FLAT AND TWO CYLINDRICAL IMPACTORS

| | | Impactor Used | |
| | Flat | Cylindrical | |
Quantity		Radius 2.54 cm [1.00 in]	Radius 1.27 cm [0.500 in]
Peak Acceleration (g_n)	90.0	63.4	62.0
Force (kN) [lbsf]*	2.26 [509]	1.57 [354]	1.42 [319]
Transducer Output (pC) side 1	157	290	340
side 2	230	670	1010
Peak Penetration (cm) (in]	0.472 [0.186]	0.762 [0.300]	0.838 [0.330]
Striker Length (cm) [in]		8.89 [3.50]	8.81 [3.47]
Footprint Area (cm^2) [in^2]	62.1 [9.62]	24.6 [3.807]	15.2 [2.354]
Average Pressure over Footprint Area (kPa) [psi]	365 [53.0]	640 [92.8]	917 [133]
Calculated Pressure at Center of Footprint (kPa) [psi]	365 [53.0]	705 [102]	926 [134]
Calculated Pressure Sensitivity			
side 1 (with negative tension contribution) (pC/Pa) [pC/psi]	4.29×10^{-4} [2.96]	4.11×10^{-4} [2.83]	3.67×10^{-4} [2.53]
side 2 (with positive tension contribution) (pC/Pa) [pC/psi]	6.31×10^{-4} [4.35]	9.49×10^{-4} [6.54]	1.09×10^{-3} [7.53]
average of sides 1 & 2 (with no tension contribution) (pC/Pa) [pC/psi]	5.31×10^{-4} [3.66]	6.82×10^{-4} [4.70]	7.25×10^{-4} [5.00]

*English unit equivalents are given in brackets.

Table 4

DROP-TEST CONDITIONS AND DATA FOR SINGLE POLYMER PRESSURE TRANSDUCER
EVALUATED WITH FLAT AND SPHERICAL IMPACTORS

Nominal drop height - 25 cm [10 in]   Gage capacitance - 913 pF
Nominal dropped mass - 2.3 kg   Cable capacitance - 132 pF

Impactor Used

Quantity	Flat	Spherical (with nominal radius of curvature of 23 cm [9 in])
Peak Force (kN) [lbsf]*	2.26 [508]	2.26 [508]
Peak Gage Output (V)	0.861	1.46
Peak Penetration (cm) [in]	0.447 [0.176]	0.579 [0.228]
Footprint Area (cm^2) [in^2]	62.1 [9.62]	62.1 [9.62]
Average Pressure over Entire Footprint Area (kPa) [psi]	364 [52.8]	364 [52.8]
Calculated Pressure at Center of Footprint (kPa) [psi]	364 [52.8]	583 [84.6]
Calculated Voltage Pressure Sensitivity (mV/Pa) [mV/psi]	2.36×10^{-3} [16.3]	2.51×10^{-3} [17.3]
Calculated Charge Pressure Sensitivity (pC/Pa) [pC/psi]	2.47×10^{-3} [17.0]	2.62×10^{-3} [18.1]

*English unit equivalents are given in brackets.
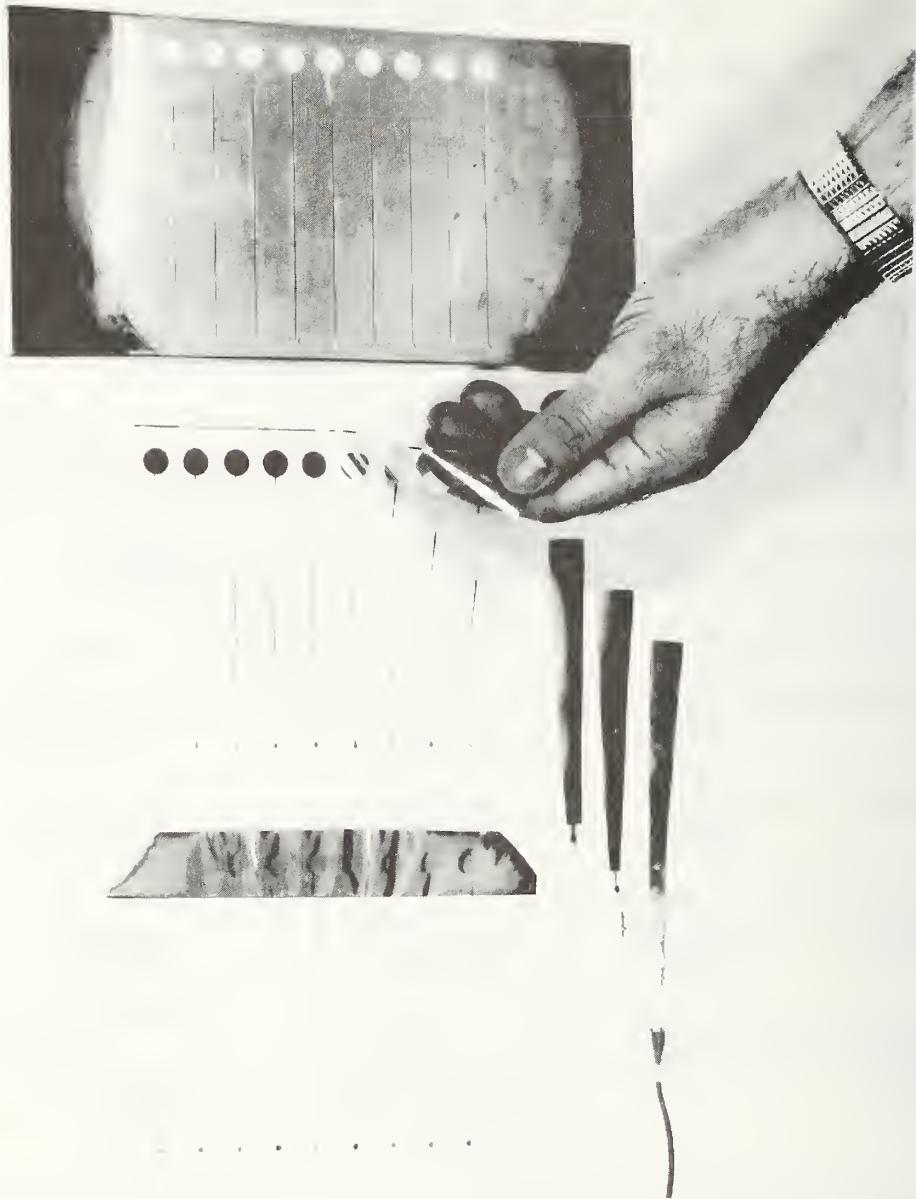
FIGURE 1: STEPS IN POLYMER PRESSURE TRANSDUCER CONSTRUCTION. AT
THE TOP IS THE MASK USED TO DEFINE THE AREAS OF THE
POLYMER SHEET THAT ARE COATED WITH ALUMINUM IN THE
VACUUM EVAPORATOR TO FORM NINE POSITIVE ELECTRODES.
THE HAND HOLDS A POLYMER SHEET WITH POSITIVE ELECTRODES
DEPOSITED. AT THE BOTTOM IS A POLYMER SHEET WITH POSI-
TIVE ELECTRODES AND A SINGLE COMMON NEGATIVE ELECTRODE.
THE NEGATIVE ELECTRODE FACES UP. THE PROCEDURE USED
TO BOND TOGETHER TWO SHEETS WITH ELECTRODES TO FORM
NINE BILAMINATE TRANSDUCER ACTIVE ELEMENTS IS DESCRIBED
IN THE TEXT. UNDER THE HAND ON THE LEFT IS A BILAMINATE
TRANSDUCER WITH A LEAD WIRE ATTACHED TO THE TWO POSITIVE
ELECTRODES. IN THE MIDDLE, THE TRANSDUCER HAS A MINIA-
TURE COAXIAL CONNECTOR ATTACHED. AT THE RIGHT IS A
FINISHED TRANSDUCER.
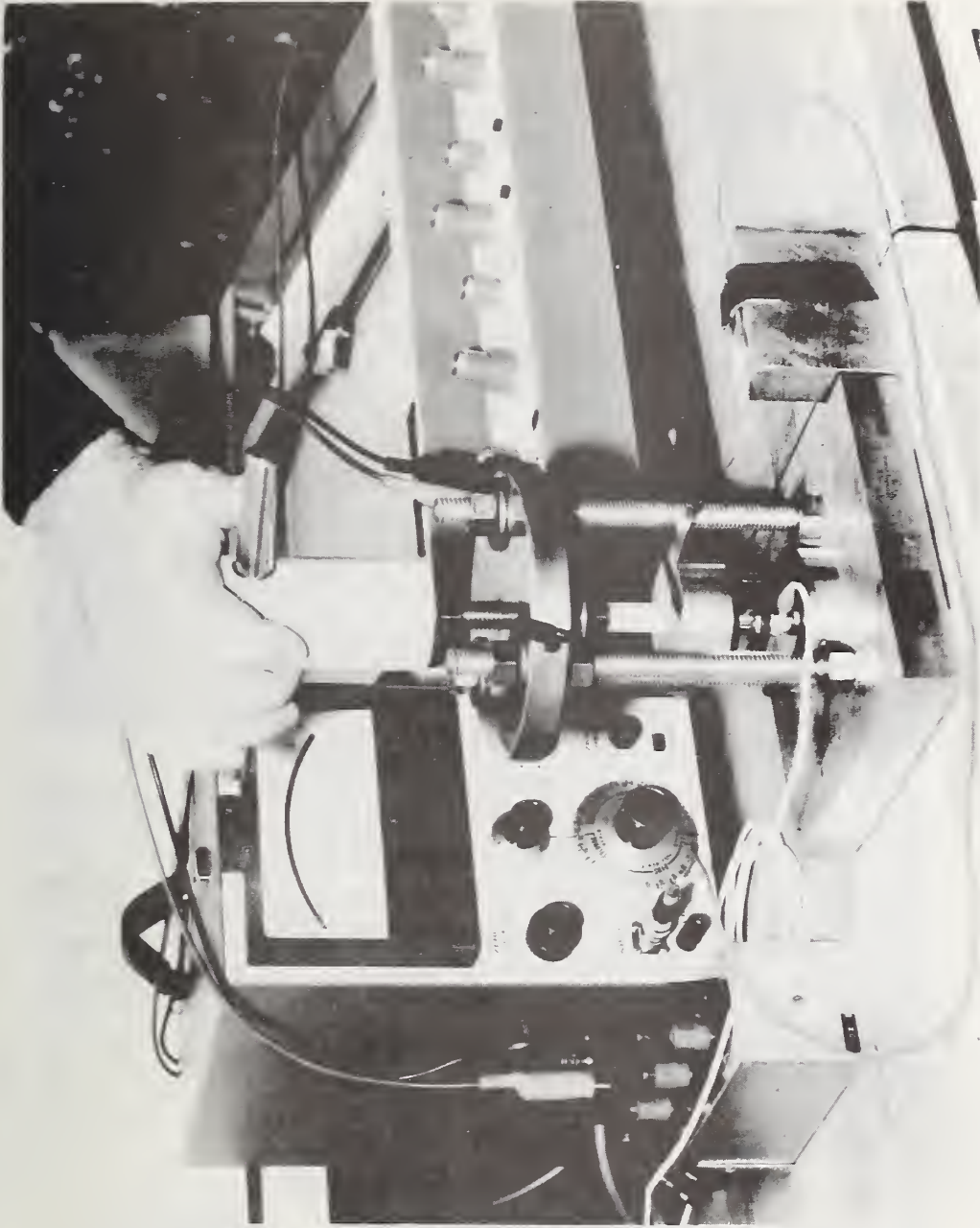
FIGURE 2: APPARATUS FOR MECHANICAL-PRESS TEST METHOD. THE COMMERCIAL FORCE TRANSDUCER (WITH WHITE LEAD) IS ABOVE THE BASE PLATE; THE POLYMER PRESSURE TRANSDUCER UNDER TEST LIES ON THE CYLINDRICAL BLOCK (SHINY) ON TOP OF THE FORCE TRANSDUCER. THE FORCE DEVELOPED BY TURNING THE HAND SCREW IS TRANSMITTED TO THE TEST TRANSDUCER BY A NYLON ROD (WHITE). THE SIGNAL FROM THE TEST TRANSDUCER IS FED TO THE INPUT OF AN ELECTROMETER (INSTRUMENT WITH DIAL); THE OUTPUT OF THE ELECTROMETER AND THE FORCE TRANSDUCER ARE PLOTTED ON AN X-Y RECORDER (INSTRUMENT AT RIGHT).
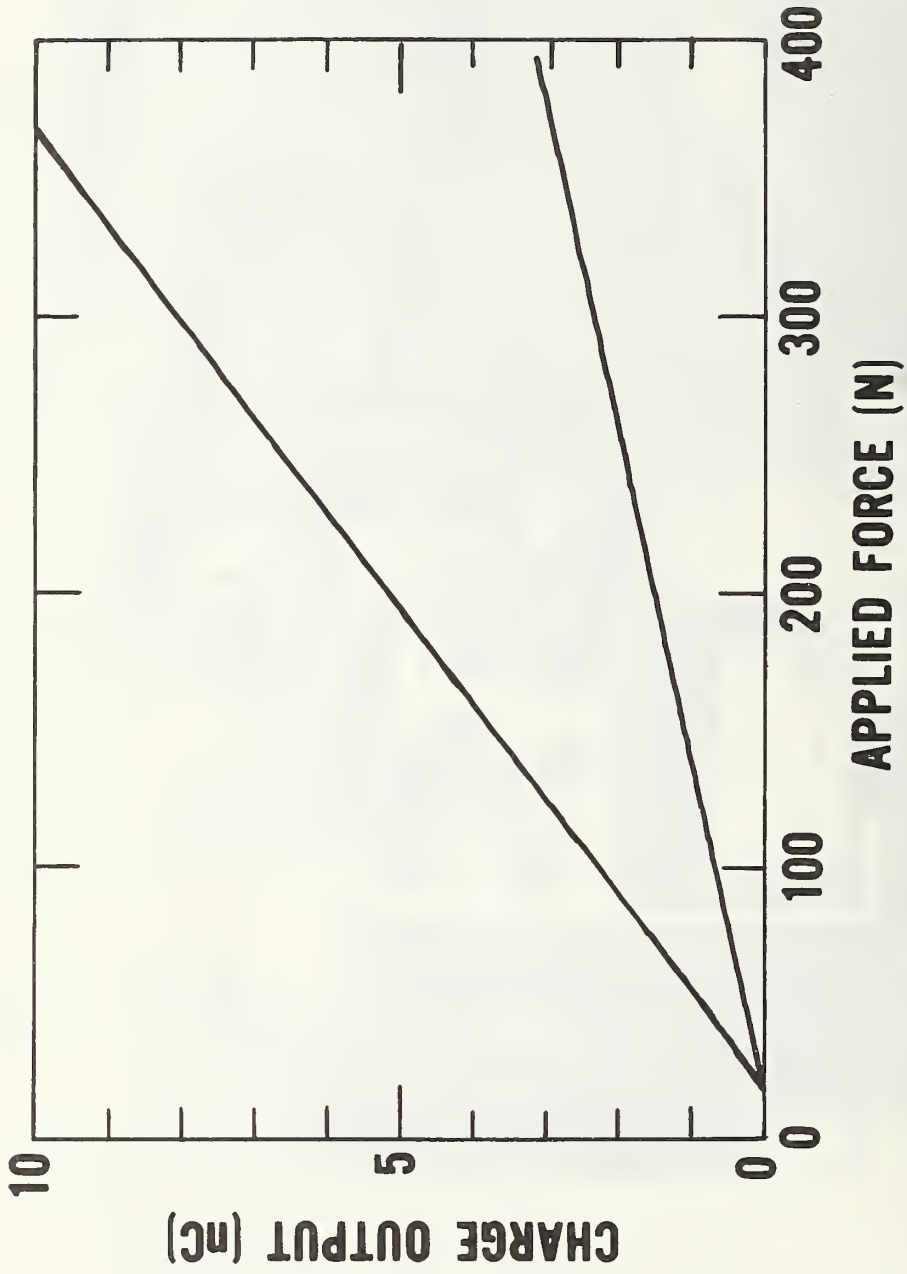
FIGURE 3: CHARGE OUTPUT (nC) VERSUS APPLIED FORCE (N) FOR TWO POLYMER TRANSDUCERS, AS OBTAINED USING THE MECHANICAL PRESS. SLOPES ARE APPROXIMATELY 28 AND 8.6 PC/N.
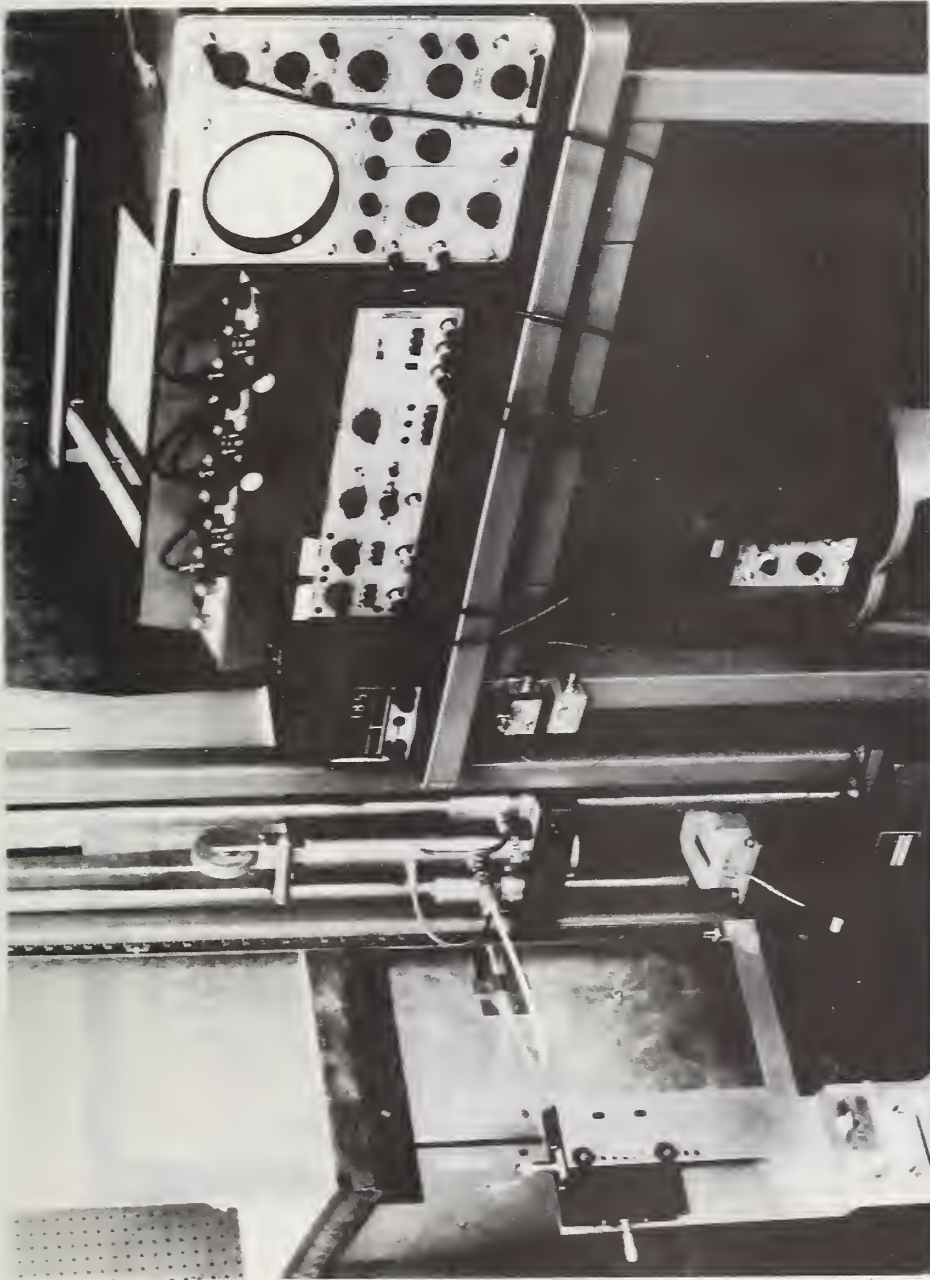
FIGURE 4: APPARATUS FOR DROP-TEST-MACHINE TEST METHOD. THE POLYMER TRANSDUCER UNDER TEST IS ON THE PAD (LIGHT COLOR) OF THE DROP-TEST MACHINE AT THE MIDDLE LEFT. A MONITORING ACCELEROMETER (WITH LEAD) IS SCREWED INTO THE UPPER FACE OF THE DROP-TEST MACHINE CARRIAGE. AN EDDY-CURRENT PROXIMITY SENSOR IS USED TO MEASURE PENETRATION DEPTH AS DESCRIBED IN THE TEXT; THIS SENSOR IS MOUNTED ON ON AN L-ARM, IN TURN MOUNTED ON A TWO-AXIS STAGE (AT FAR LEFT). THE OUTPUTS FROM BOTH ACCELEROMETER AND TEST TRANSDUCER ARE STORED, MONITORED, PROCESSED, AND RECORDED BY MEANS OF THE OTHER INSTRUMENTATION SHOWN.
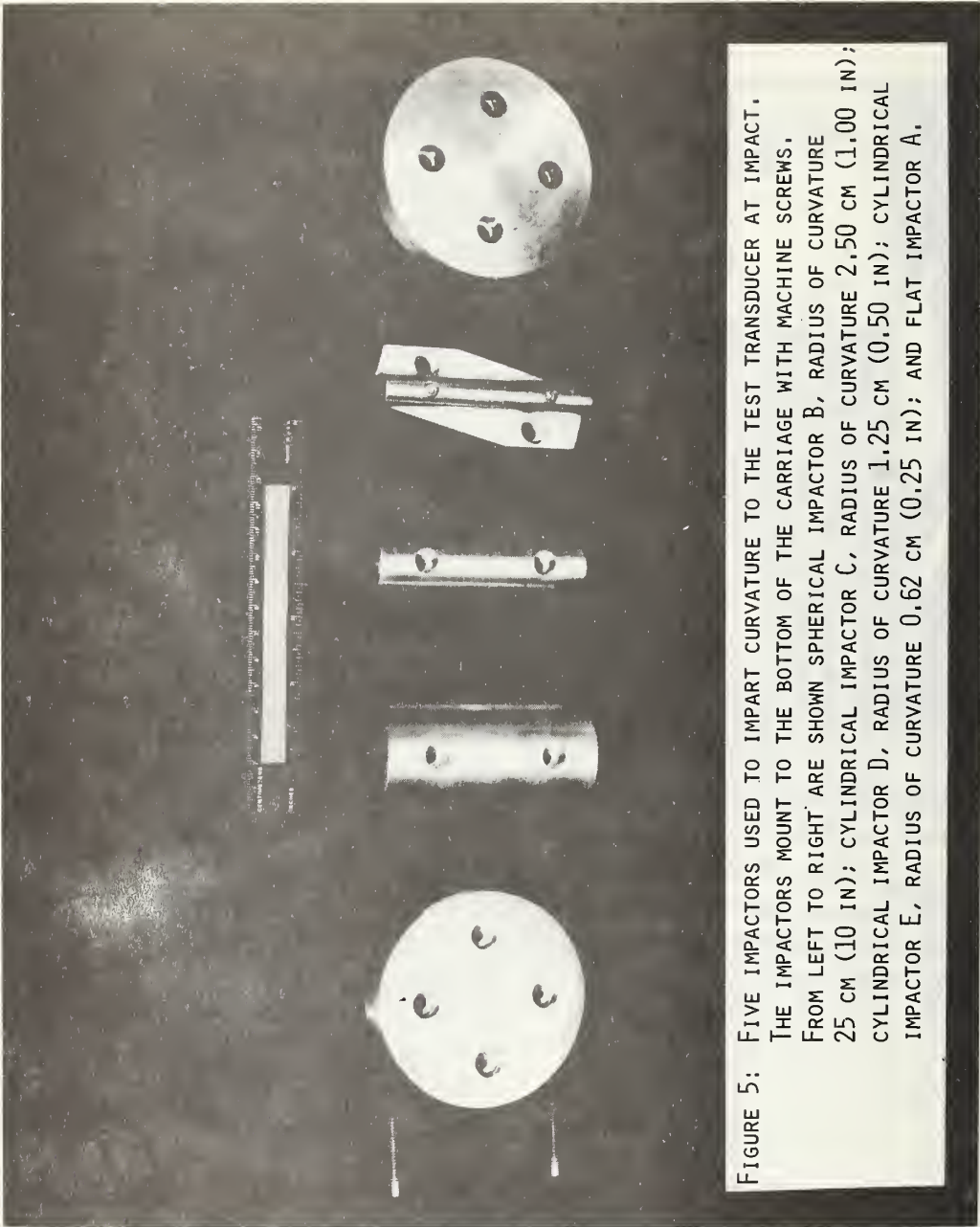
FIGURE 5: FIVE IMPACTORS USED TO IMPART CURVATURE TO THE TEST TRANSDUCER AT IMPACT. THE IMPACTORS MOUNT TO THE BOTTOM OF THE CARRIAGE WITH MACHINE SCREWS. FROM LEFT TO RIGHT ARE SHOWN SPHERICAL IMPACTOR B, RADIUS OF CURVATURE 25 CM (10 IN); CYLINDRICAL IMPACTOR C, RADIUS OF CURVATURE 2.50 CM (1.00 IN); CYLINDRICAL IMPACTOR D, RADIUS OF CURVATURE 1.25 CM (0.50 IN); CYLINDRICAL IMPACTOR E, RADIUS OF CURVATURE 0.62 CM (0.25 IN); AND FLAT IMPACTOR A.
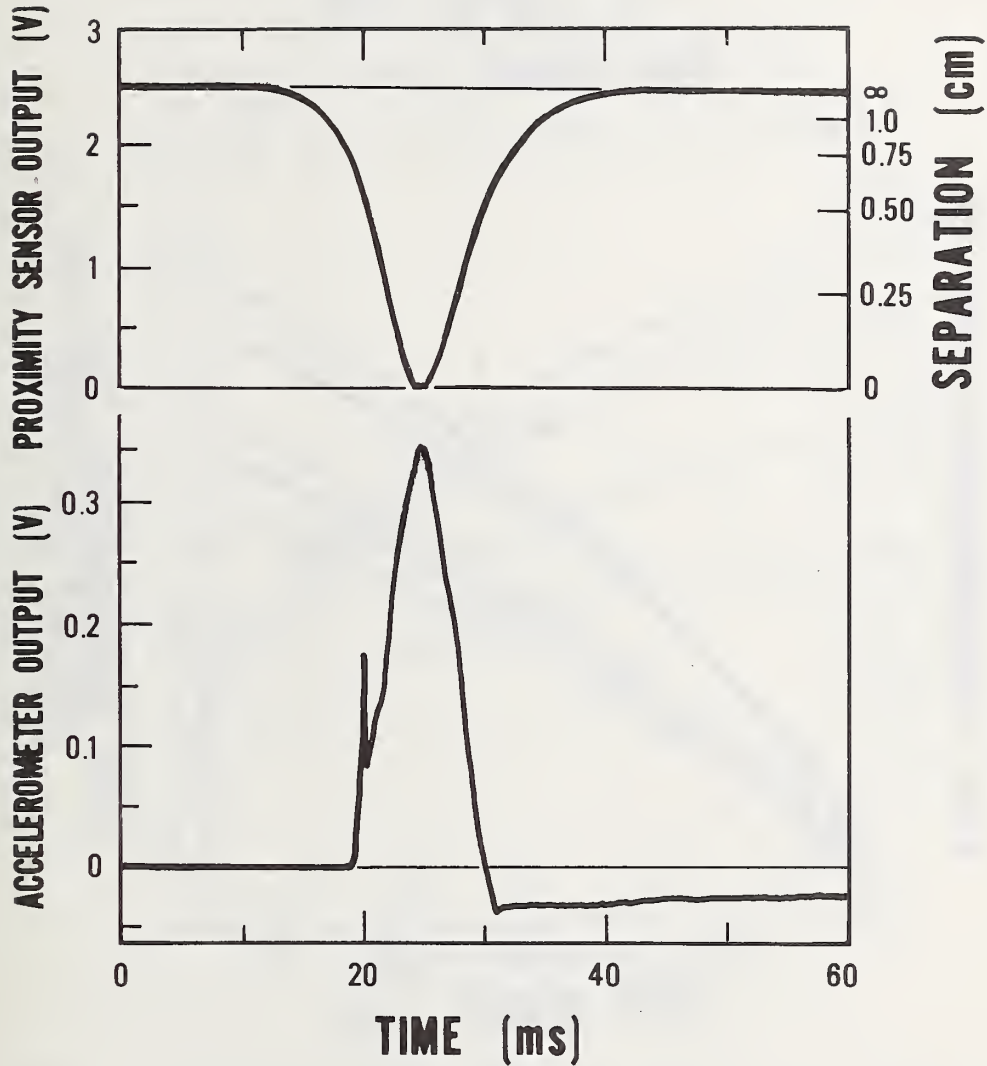
FIGURE 6: PROXIMITY SENSOR OUTPUT (V) AS A FUNCTION OF TIME (UPPER PANEL) AND ACCELEROMETER OUTPUT (V) AS A FUNCTION OF TIME (LOWER PANEL) FOR 2.5-KG (5.5-LB MASS) MASS CARRIAGE WITH FLAT IMPACTOR AT 13-CM (5 IN) DROP HEIGHT. RECORDED TRACES ARE SHOWN. AT THE RIGHT OF THE UPPER PANEL IS A CALIBRATION SCALE FOR THE SEPARATION BETWEEN TARGET AND PROXIMITY SENSOR (CM).
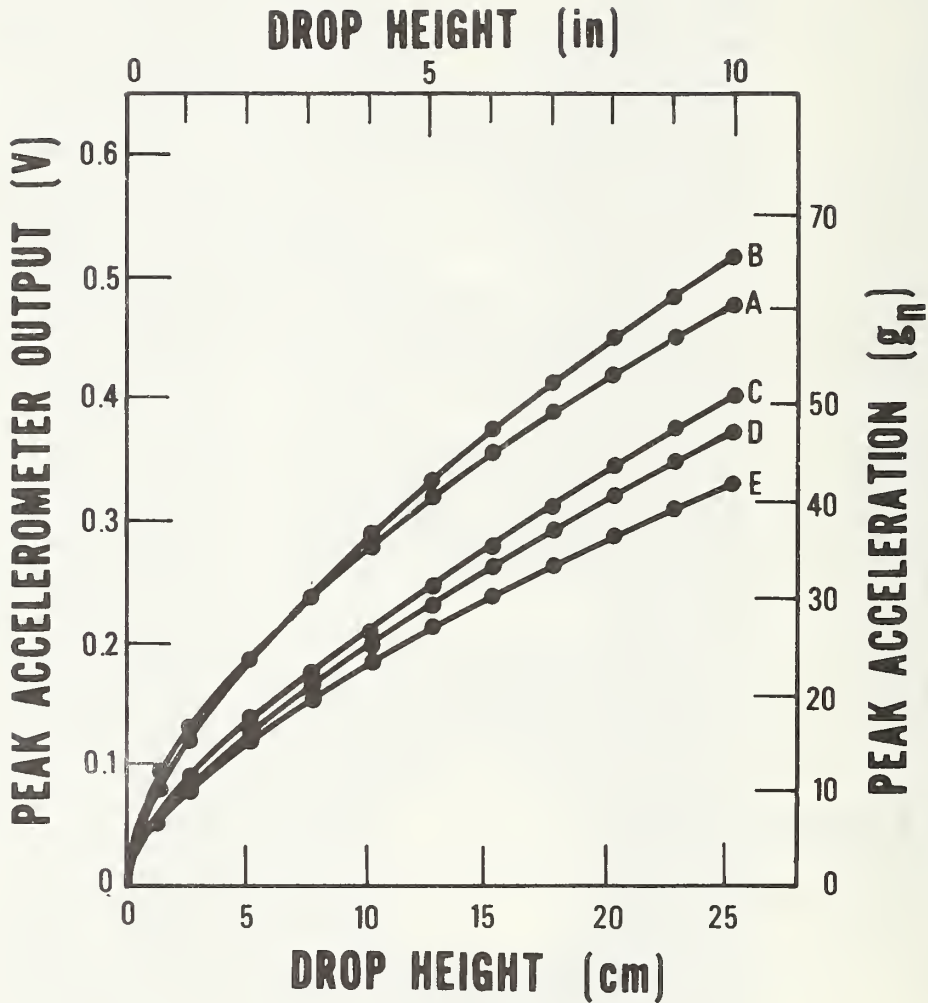
FIGURE 7: PEAK ACCELEROMETER OUTPUT (V) AS A FUNCTION OF DROP
HEIGHT (CM AND IN) FOR FIVE IMPACTORS, A-E. IMPACTORS
ARE IDENTIFIED IN THE CAPTION OF FIGURE 5 AND IN TABLE 1.
THE CARRIAGE MASS WAS 2.5 KG (5.5 LB MASS); A FLAT-
SURFACED HALF-SINE PAD WAS USED ON THE ANVIL, AS DESCRIBED
IN THE TEXT. A CALIBRATION SCALE IN UNITS OF PEAK ACCEL-
ERATION (g_n) FOR THE ACCELEROMETER OUTPUT IS GIVEN AT THE
RIGHT.
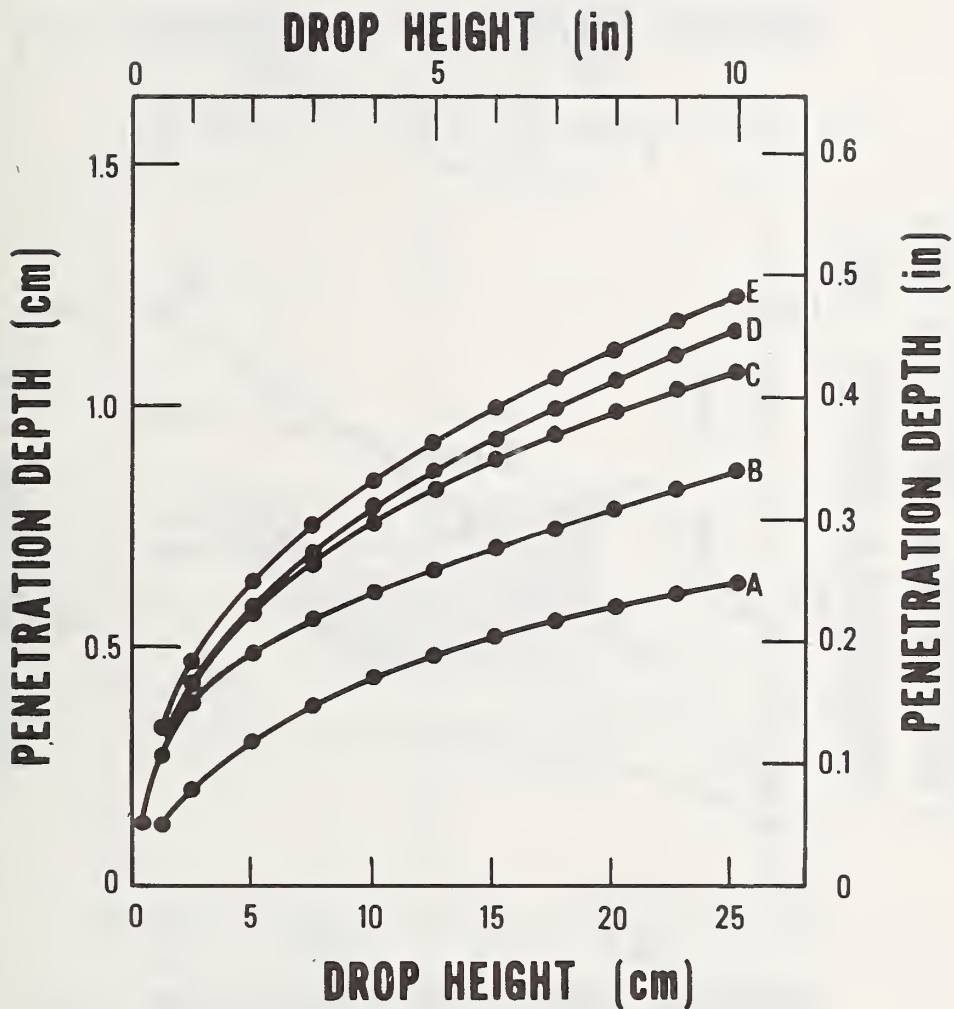
FIGURE 8:   PENETRATION DEPTH (CM AND IN) AS A FUNCTION OF DROP
            HEIGHT (CM AND IN) FOR FIVE IMPACTORS, A-E.   IMPACTORS
            ARE IDENTIFIED IN THE CAPTION OF FIGURE 5 AND IN
            TABLE 1.   THE CARRIAGE MASS WAS 2.5 KG (5.5 LB MASS);
            A FLAT-SURFACED HALF-SINE PAD WAS USED ON THE ANVIL,
            AS DESCRIBED IN THE TEXT.
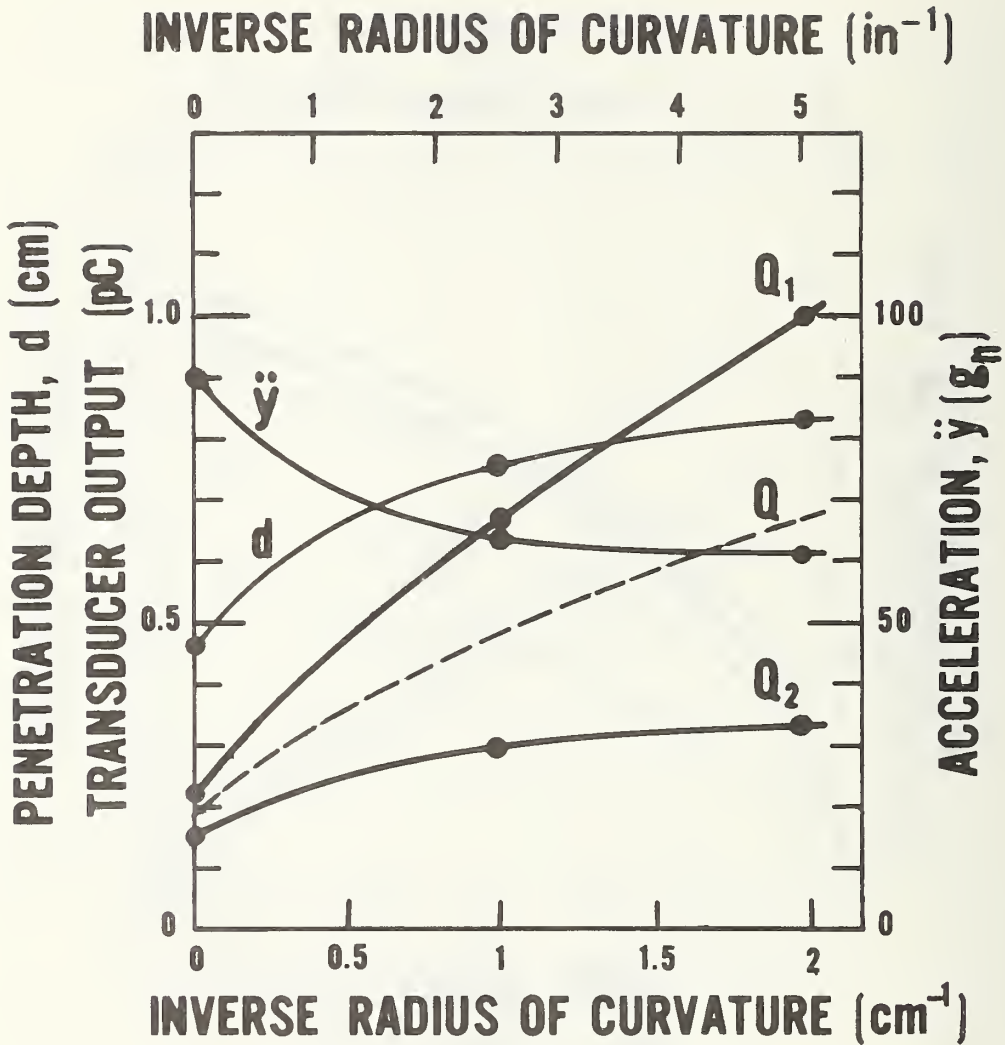
FIGURE 9: PEAK POLYMER PRESSURE TRANSDUCER OUTPUT, CURVES Q1, Q2, AND Q (NC); ABSOLUTE MAGNITUDE OF PEAK ACCELERATION, CURVE $\ddot{y}$ (g_n); AND PEAK PENETRATION DEPTH, CURVE d (CM) AS FUNCTIONS OF INVERSE IMPARTED RADIUS OF CURVATURE (CM), FOR CYLINDRICAL CURVATURE. THE CURVES HAVE BEEN FITTED BY EYE TO THE EXPERIMENTAL POINTS SHOWN. Q1 REPRESENTS TRANSDUCER OUTPUT WHEN SIDE 1 IS FACING UPWARDS, Q2 REPRESENTS TRANSDUCER OUTPUT WHEN SIDE 2 IS FACING UPWARDS, AND Q IS THE AVERAGE OF Q1 AND Q2. THE DATA REFER TO A SPECIFIC TRANSDUCER TESTED WITH SPECIFIC DROP-TEST CONDITIONS, AS DESCRIBED IN 4.2.1.
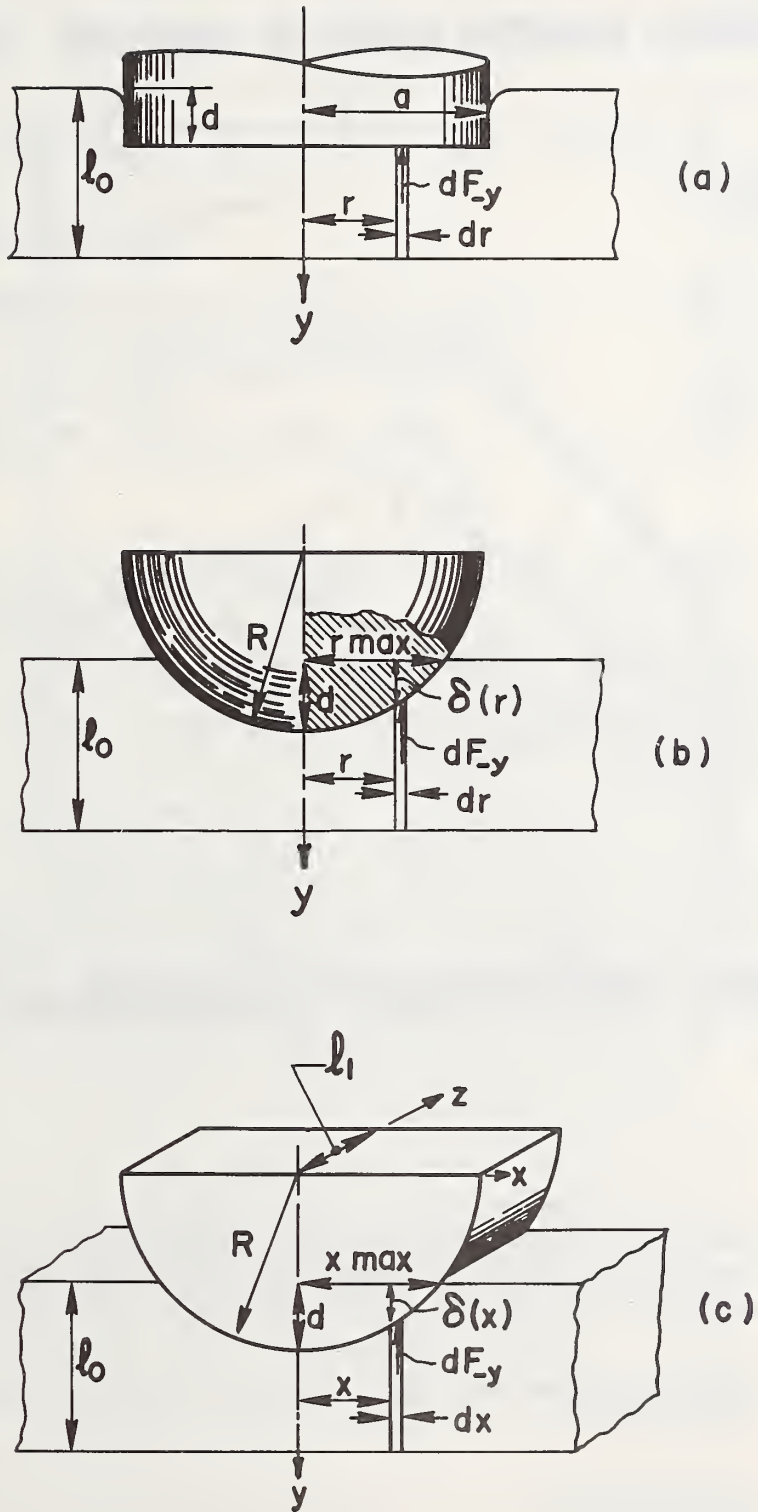
FIGURE 10: IMPACT GEOMETRY FOR (A) FLAT IMPACTOR, (B) SPHERICAL IMPACTOR, AND (C) CYLINDRICAL IMPACTOR. THE MEANING OF THE LABELS IS DESCRIBED IN THE TEXT.
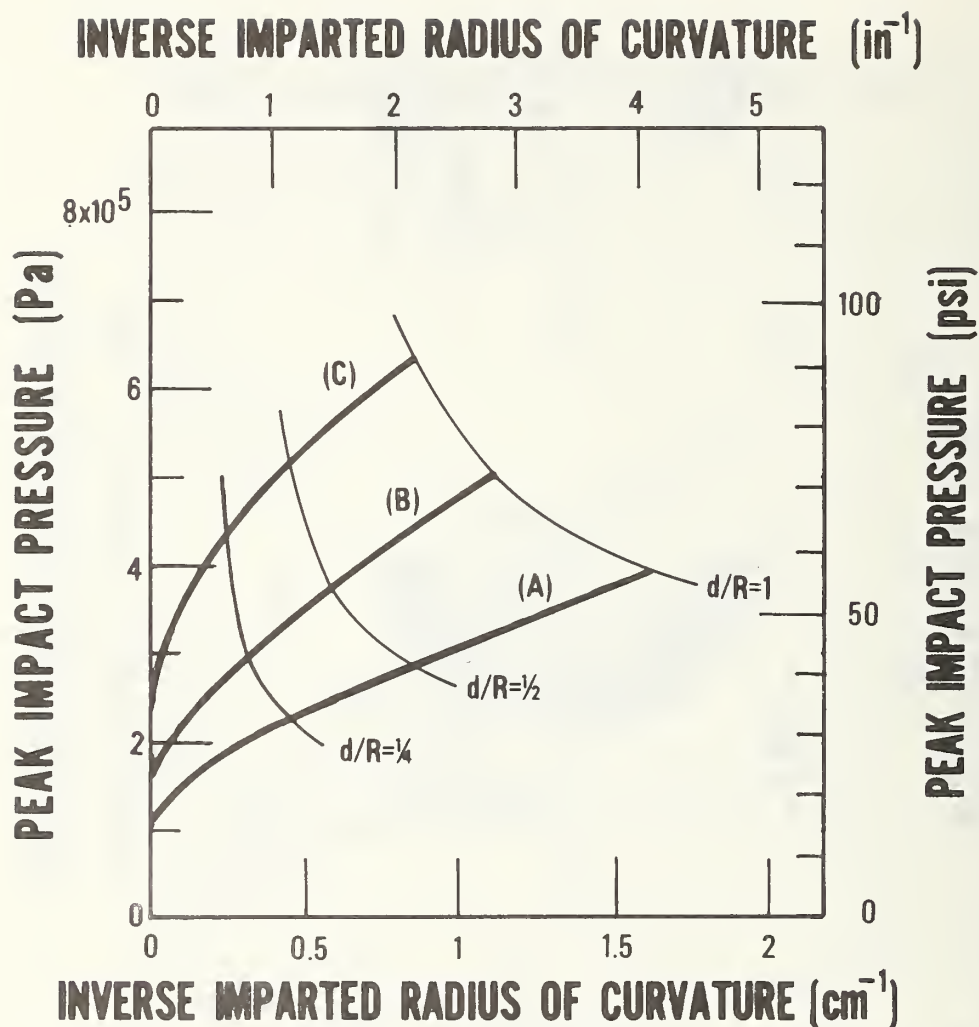
FIGURE 11: PEAK IMPACT PRESSURE (PA AND PSI) AS A FUNCTION OF THE INVERSE IMPARTED RADIUS OF CURVATURE (CM^{-1} AND IN^{-1}), OF THE CYLINDRICAL IMPACTOR, FOR THREE DROP HEIGHTS. THE CURVES WERE PLOTTED FROM CALCULATED VALUES, AS DESCRIBED IN THE TEXT. CURVE A IS FOR A DROP HEIGHT OF 5.2 CM (2.0 IN); B, 12.7 CM (5.0 IN); AND C, 25.4 CM (10.0 IN). CONSTANT D/R CONTOURS (LINES OF CONSTANT PENETRATION DEPTH/RADIUS OF CURVATURE) ARE ALSO SHOWN.

U.S. DEPT. OF COMM. BIBLIOGRAPHIC DATA SHEET	1. PUBLICATION OR REPORT NO. NBSIR 75-740	2. Gov't Accession No.	3. Recipient's Accession No.

4. TITLE AND SUBTITLE	5. Publication Date
Piezoelectric Polymer Transducer for Impact Pressure Measurement	July 1975
	6. Performing Organization Code

7. AUTHOR(S) Aime S. DeReggi	8. Performing Organ. Report No.

9. PERFORMING ORGANIZATION NAME AND ADDRESS	10. Project/Task/Work Unit No.
NATIONAL BUREAU OF STANDARDS DEPARTMENT OF COMMERCE WASHINGTON, D.C. 20234	4253560
	11. Contract/Grant No. DOT-HS-4-00835

12. Sponsoring Organization Name and Complete Address (Street, City, State, ZIP)	13. Type of Report & Period Covered
Office of Vehicle Safety Research and Development National Highway Traffic Safety Administration Department of Transportation 400 Seventh Street, SW, Washington, D.C. 20590	12/15/73-12/31/74
	14. Sponsoring Agency Code

15. SUPPLEMENTARY NOTES

16. ABSTRACT *(A 200-word or less factual summary of most significant information. If document includes a significant bibliography or literature survey, mention it here.)*

Described are development efforts relating to the design, construction, and calibration of a piezoelectric polymer transducer for the recording of pressure transients developed over the interface between two bodies as a result of impact. A bilaminate design was selected which uses electrically poled sheets of 25-μm poly(vinylidene fluoride) as the active material. The intended primary response of the transducer is to compression in the thickness direction, which is produced by either hydrostatic or normal pressure; the transducer was also found to respond to extension in the membrane direction. Individual-sheet activity in the thickness-compression mode is approximately 15 pC/N, resulting in a bilaminate transducer pressure response of 4.5 μV/Pa(30 mV/psi). Instructions for poling sheets and for constructing transducers are given in detail. Static and dynamic methods for characterizing transducer output are described. In particular, in order to simulate field conditions in which the transducer may bend or stretch, or both, during impacts, a drop-test procedure with curved impactors has been devised and a theoretical analysis (simplified to the extent of considering the membrane-stress contribution negligible) has been developed to yield the interface pressure.

17. KEY WORDS *(six to twelve entries; alphabetical order; capitalize only the first letter of the first key word unless a proper name; separated by semicolons)* Calibration; construction; impact; interface; piezoelectric polymer; polymer; pressure; pressure transducer; theory; transducer.

18. AVAILABILITY ☒ Unlimited	19. SECURITY CLASS (THIS REPORT)	21. NO. OF PAGES
☐ For Official Distribution. Do Not Release to NTIS	UNCLASSIFIED	37
☐ Order From Sup. of Doc., U.S. Government Printing Office Washington, D.C. 20402, SD Cat. No. C13	20. SECURITY CLASS (THIS PAGE)	22. Price
☐ Order From National Technical Information Service (NTIS) Springfield, Virginia 22151	UNCLASSIFIED	